Photodeposition of Palladium Supported on TiO2 Nanotubes Powder as Electro Catalyst for Methanol Oxidation Reaction

*Mohammed .A.H.Awad ** Nabil A.N. Alkadasi ***Abdullah .M. Al-Mayouf

Abstract

Titanium oxide nanotubes powder (TONTs powder) was prepared by hydrothermal method into annealed in N2 at 450°C for 3 hours to obtain the TONTs-N2 powder as catalyst support to which Pd was loaded by photodeposition technique using PdCl2 and isopropanol as sacrificial donor. The resulting Pd-TONTs-N2 powder catalyst improved high surface area of 177 m2/g. The physicochemical characterization of TONTs arrays powder were performed by X-ray diffraction (XRD), scanning electron microscopy (SEM), transmission electron microscopy (TEM), and surface area and pore size analysis. The catalyst support TONTs arrays powder were electrochemically characterized in basic solution of methanol by cyclic voltammetry (CV), and chronoamperometry measurements.Pd-TONTs-N2 powder electrode catalyst exhibited a remarkably high electrocatalytic activity and has high electrocatalytic stability for methanol electrocatalytic oxidation reaction. Pd supported on the conductive support TONTs-N2 is used as electrocatalyst in fuel cells.

Key words:

Methanol oxidation reaction (MOR), titanium oxide nanotubes powder, photodeposition, Pd electro catalyst, chronoamperometry.

1. Introduction

In the previou work "Palladium supported on titanium oxide nanoparticles as a catalyst for methanol oxidation reaction "was synthesised [1]. Titanium oxide nanotubes (TONTs) are

of specific importance due to their greater physicochemical properties and potential applications in electro catalysis [2], photocatalysis [3, 4], solar energy cell, environmental purification, gas sensors [5], energy usage containing H2 storage and batteries of lithium. (TONTs) arrays have attracted much interest due to their large specific surface area, chemistry positive surface, and best biocompatibility [6].

Hydrothermal synthesis of TiO2 nanotubes powder (TONTs powder) by using two steps including sonication

*Chemistry Department, Faculty of Applied Sciences , Thamar University.
**Faculty of Engineering, Thamar University.
*** Chemistry Department, College of Sciences ,King Saud University.

process and static hydrothermal process to

fabricate the TiO2 nanotubes [7-9].The Pd-TONTs-N2 powder fabricated by photodeposition method by means of 400 W UV. The radiation with UV was suitable for Pd to reduce and deposit onto the surface of titanium oxide nanotubes powder. Hence, offer a sustainable synthesis method. This was attained during expositing catalyst supported to 400 W UV, through which free electrons holes were produced. The electrons were excited into the conduction band (CB) which functions as an electron source for the palladium cations reduction. The photoelectrons produced by dint of titanium oxide nanotubes reduce the Pd2+ cation to palladium metal nanoparticles. In the meantime, the photogenerated holes from

valance band (VB) react with isopropanol to form aldehyde [10-14]. The whole mechanism was shown in Fig.1. The synthesized TONTs displayed absolutely the anatase phase. On the other hand, the UV leads to the reduction and fixing of palladium nanoparticles onto the surface of TONTs-N2 powder.

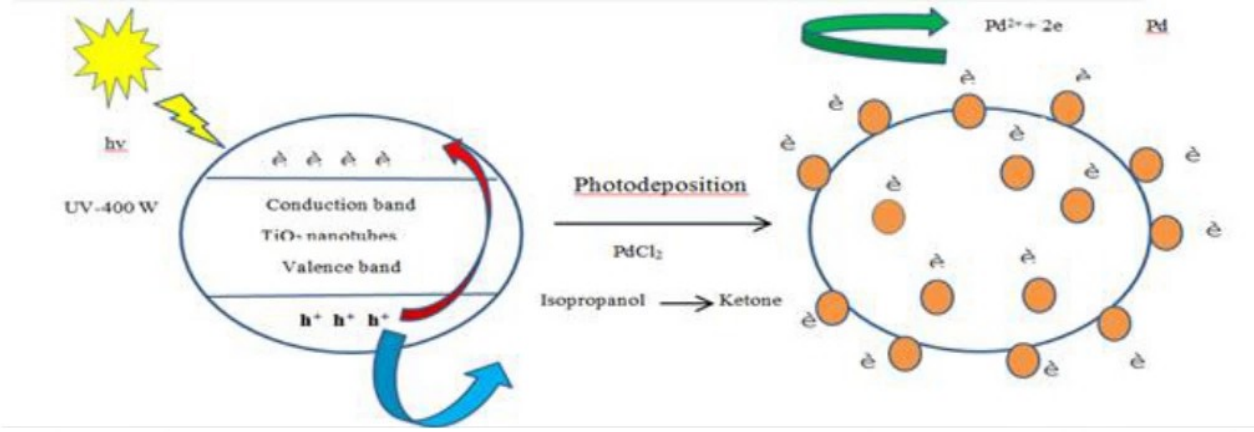

Fig.1: Mechanism of palladium photodeposition (Illustrated drawing for the preparation of Pd-TONTs-N2 catalyst using UV-400 W lamp photodeposition).

2. Experiment

2.1 Materials

Ti foils (>99.5% purity, Alfa Aesar, thickness: 0.25 mm), perchloric acid HClO4 Palladium (II) chloride (PdCl2, Sigma– Aldrich, 99.9+ %) as precursor, isopropanol (99.0 %) as sacrificial donor, TONPs powder prepared in our lab (surface area 109m²/g), Nafion (5 wt %).

2.2 Synthesis of TONPs powder

At the beginning titanium oxide nanoparticles powder (TONPs powder) was prepared by the electrochemical anodic oxidation (annodization process). The Ti foils (>99.5% purity, Alfa Aesar, thickness: 0.25 mm) were anodized in an aqueous solution containing 0.7 M perchloric acid HClO4 using a two-electrode electrochemical cell (Ti foil as

the anode and Pt foil as the cathode) at 20V for 1h at room temperature then, we separate the precipitate (TONPs powder) from the mixed solution using 7000 rpm centrifuge. Then dry the precipitate in oven at 80 °C for overnight, then use pestle and mortar to make smooth powder to obtain TONPs powder.

Hydrothermal synthesis of TiO2 nanotubes powder (TONTs powder)

Synthesis of TiO2 nanotubes, 2 g of the TONPs powder (prepared in our lab) was mixed with 100 ml of 10 M NaOH and the suspension system was stirred for 1h at room temperature to form a suspension. The hydrothermal treatment of the mixture was carried out at 150°C for 24 hours in autoclave. When the reaction was completed, the white solid was collected and washed using 200 ml of 0.1 M HCl followed with deionized water till a pH 7 of wash solution was obtained. The last products were obtained by means of 7000 rpm centrifuge with consequent drying at 80 °C for 24 hours. The TONTs powders were subsequently annealed at 450 °C in N2 for 3hours with heating and cooling rates of 5 °C min−1 to obtain TONTs-N2 powder.

Photodeposition by UV-400W lamp was carried out in an aqueous solution contains 150 mg of TONTs powder, 10 ml of 20 mM PdCl2, 10 ml of 0.3 M isopropanol and put in the beaker magnetic stirrer for 2hs. In this step we note change in the colour of the solution in the case of palladium from the yellow colour to the light green colour and this prooks that palladium is deposited on the surface of TONTs-N2 powder. Then, we separate the precipitate (e.g. Pd adsorbed on TONTs-N2 powder) from the mixed solution using centrifuge. Then dry the precipitate in an oven at 80 °C for overnight, then use pestle and mortar to make smooth powder. Then to prepare the ink; weigh 50 mg of (Pd-TONTs-N2 powder) and add to it 1ml DI water plus 20 µL of nafion (5 wt. %) solution to stick the catalyst on the Au working electrode. After that, we loaded 3 µl of the catalyst (Pd-TONTs-N2 powder) by micropipette on 3 mm Au polycrystalline working electrode to carry out cyclic voltammetry (CV).

2.4 Physicochemical characterizations

Transmission electron microscopy (TEM) images were obtained using a JEOL JEM-2100F electron microscope operating at 200 kV.

X-ray diffraction (XRD) data were collected on a Model RIGAKU MINIFLEX 100 X-ray diffract meter, operating at tube voltage 40 kV and tube current 15 mA, using Cu(Kα) , intensity was 0-400 cps , range of 2θ(deg) was 5-80 degree i.e. wide angle. For chilling, the water flow rate was 3.7 L/min, scan rate either 5 °/min or 2 °/min. Monochromator is used.

BET (Brunauer-Emmett-Teller) surface area and porosity measurements were

carried out by N2 adsorption at 77.3 K using Quantachrome instrument.

2.5 Electrochemical measurements

Cyclic Voltammetry (CV)

CV was performed in a conventional three-electrode single-compartment Pyrex glass cell using a computerized potentiostat/galvanostat (Autolab, FRA2, µAUTOLAB, TYPE III). The reference and auxiliary electrodes were SCE and pure Pt-foil, respectively. All potentials provided in the text are based on the SCE electrode only. A Pt wire auxiliary electrode and a saturated calomel reference electrode (SCE) were used. Also 3mm Au polycrystalline working electrode was used (with geometric surface 0.07 cm2).The software program used in cyclic voltammetry measurements were NOVA 1.9. An evenly distributed suspension ink of catalyst was prepared by ultrasonic the mixture of 50 mg catalyst and 1 mL D.I water for 30 min, and 3 µL of the resultant suspension was laid on the surface of Au polycrystalline working electrode (3 mm diameter, 0.07 cm2). After drying at 40 °C, 1 µL of Nafion (5 wt. %) solution was covered on the catalyst surface and allowed to dry again. Thus, the working electrode was obtained, and the specific loading of metal on the Au working electrode surface was about 0.0225 mg (22.5µg). Electrochemical tests were performed in 2 M KOH + different concentrations of methanol.

Chronoamperometry (CA) was carried out in different potentials i.e. at -0.4V,-0.27V, and 0V.

Material characterization

The mass loading of the (metals) Pd in the prepared materials were determined by means of an inductively coupled plasma spectroscopy system (ICPS-7000 ver.2 Shimadzu, SEQUENTIAL PLASMA SPECTROMETER). For that, determination, samples were dissolved in aqua regia (3HCl: 1HNO3) (E-Merck) acid by means of high-pressure microwave digestion in Teflon tube vessel system (MARSX; CEM) at 450K and 170 psi. The Microwave Accelerated Reaction System (MARS) was used.

3. Results and discussion

3.1Physicochemical Characterization of Pd-TONTs-N2 powder catalyst

Fig. 2 showed the TONTs-N2 powder catalyst support before treated with UV radiation and after 2 hours illimination by 400 W UV in precenced of palladium solution and obtaining Pd-TONTs-N2 powder electrocatalyst. The changes in color (from white color to yellow color) was observed un treated and treatment.

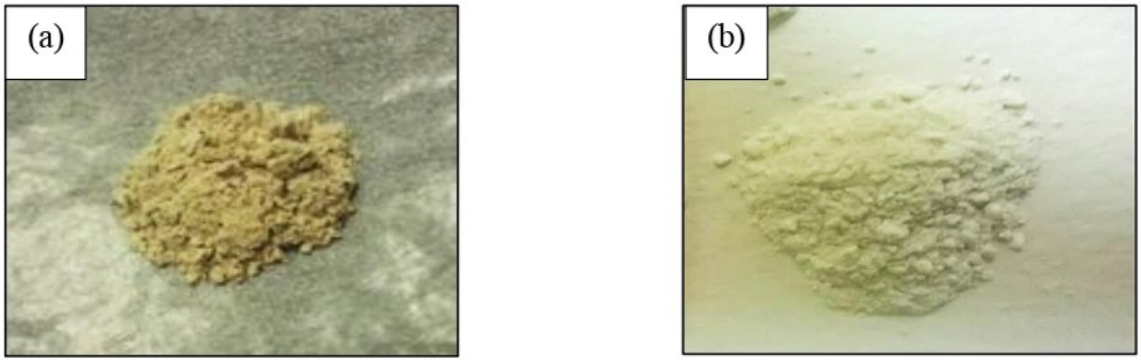

Fig. 2: (a) TONTs powder before photodeposition and (b) Pd-TONTs-N2 powder after photodeposition.

Fig. 3 exhibit SEM image of TONTs sample synthesized at 150 °C for 24 h before and after washing. Fig. 3a reveals that the starting TONPs powder particles had been fully transformed into nanotubes before washing at 150 °C in 24 h. Thus, during heating process of reaction from room temperature to 150°C, the nanotubes were formed. The length of nanotubes increased corresponding to the reaction time, and the uniformed wire-like nanotubes were obtained in the sample without washing in the dynamic hydrothermal time of 24 h as shown in Fig. 3 b. This result indicates that the nanotubes are formed during the dynamic hydrothermal process and definitely contradicts the assumption that titanate precursor sheets would only scroll after acid treatment [15].The microstructure of nanotubes before and after washing can be found to be similar in comparison Fig. 3a with Fig. 3b. In this study, TONPs powder was the precursor of the synthesized TONTs powder [16].

The SEM images of the samples prepared in a concentrated NaOH treatment and with a subsequent acid washing then DI water until obtain pH=7 of filtrate are shown in Fig. 3. Fig. 3a is the microscopic figure with low-power field (magnification 50,000 times). We can observe that the uniformity of the structure distribution inside the catalyst support is very excellent, and no particle is remained because of the incomplete reaction. As clearly seen from Fig. 3 a and b numerous fiber like nanotubes grow from nano-size TONPs powder. It,s group is like a petal with bunchy arrangement not disarray. Under these conditions, the outer diameter and length of the nanotubes is about 10 nm and >1μm respectively [17]. The TONTs made from TONPs powder could improve significantly the specific surface area, increase the efficiency of electron transport and also separate the electron-hole pairs efficiently.

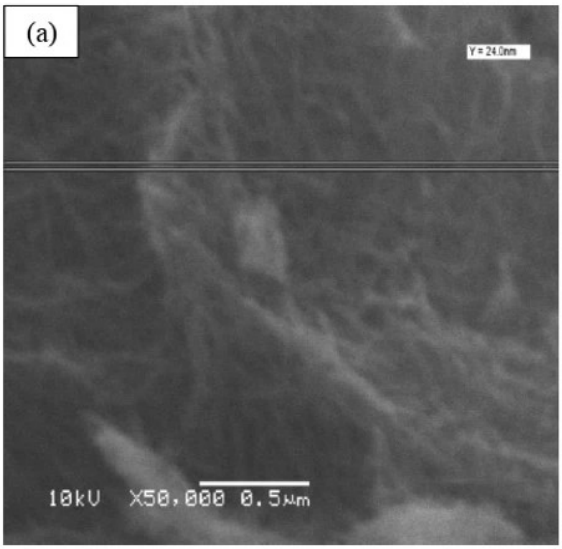

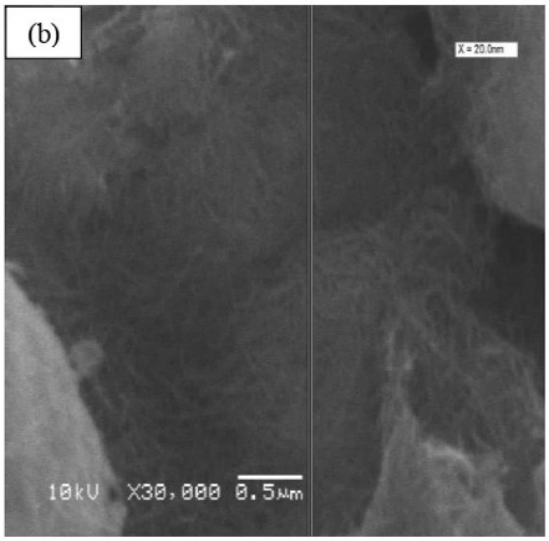

Fig. 3: The SEM image of TONTs prepared from a 10 M NaOH treatment at 150 °C and with a subsequent acid washing then DI water until obtain pH=7 of filtrate. (a) magnification of 50,000 times before washing treatment, (b) magnification of 30,000 times after washing treatment. Scale was 0.5 µm (500 nm).

Fig. 4 shows TEM images of TONTs befor washing , after washing with 1.0 M HCl and after calcination in 450 °C for 3h.The nanotubes are observed as shown in Fig. 4 (a) (b) and (c), and (d) indicating that nanotubes had scrolled into nanotubes before washing. TiO2 samples after washing was still nanotubes (as shown in Fig. 4 c). In comparison to Fig. 4 a and b, it can be found in Fig. 4c that the nanotubes before and after calcination were similar. The results of TEM indicated that crystalline phase of TiO2 nanotubes transformed from titanate into anatase phase after calcination in 3h at 450 °C,whereas the microstructure of nanotubes was not changed. The complete nanotubes structure was obviously detected in the 150 °C sample The average outer diameter and the length of the nanotubes formed at 150 °C are about 12 and 110 nm, respectively [18].

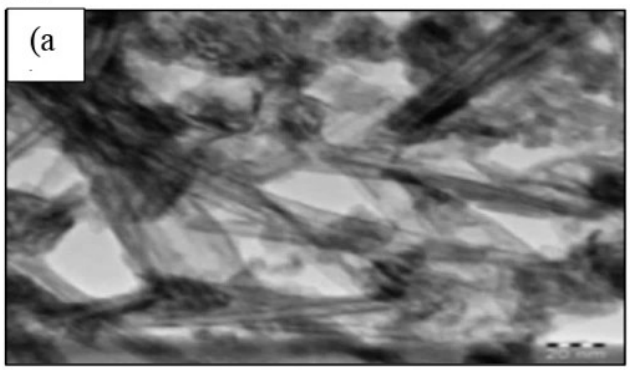

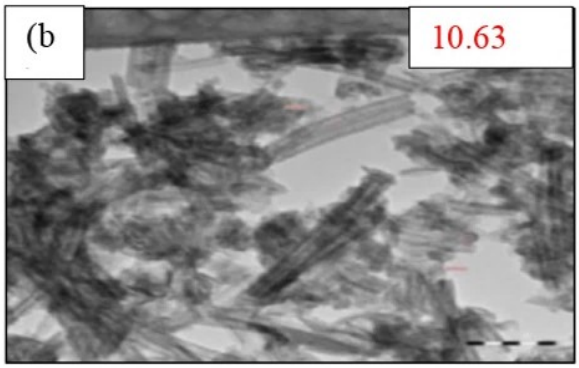

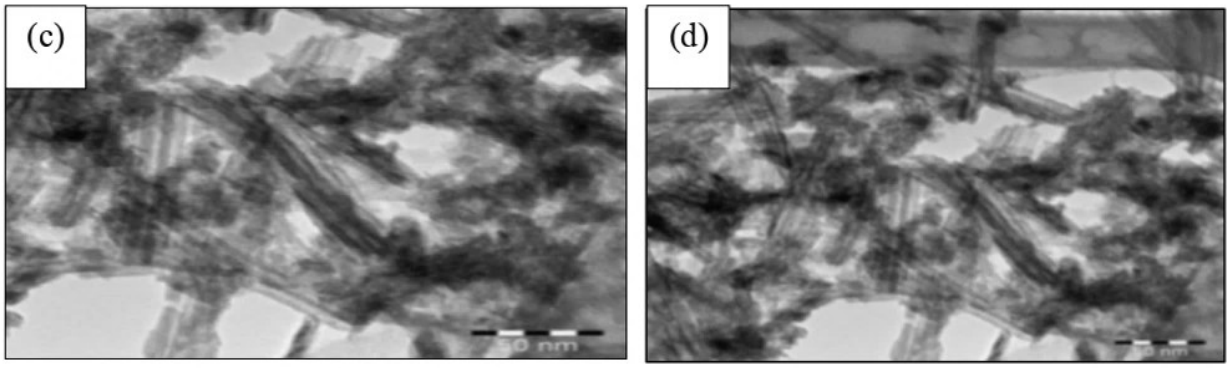

Fig. 4: TEM image of TONTs powder (a) 20 nm and (b) 50 nm before washing (c) 50 nm after washing (d) 50 nm after calcination in 450 °C for 3h. The distance between two nanotubes is 10.63 nm.

Fig. 5 shows the XRD pattern for the TONTs powder array via annealing at 450 °C (TONTs-N2) for 3h. The diffraction peaks of TONTs array agree with the standard JCPDS anatase cards TiO2 (No. 21-1272). The XRD pattern of the TONTs arrays displays (101), (004), (200), (105), (211), (116), (204), (220) and (215)anatase peaks.

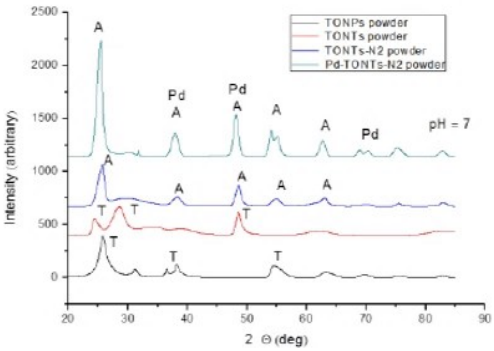

Fig. 5: XRD patterns of TONPs powder, TONTs powder after washing, TONTs-N2 powder (after calcination at 450°C for 3h) and Pd-TONTs-N2 powder.

The major diffraction peaks of the as-synthesized sodium nanotubes and protonated titanate nanotubes obtained by acid treatment (before calcination at 450 °C for 3 h) and the final anatase TiO2 nanotubes (after calcination at 450 °C for 3 h) sample found at 2□ ~ 10.2°.24.2°, 28.4°, and 48.3° were characteristic of the tubular Na2Ti3O7 (JCPDs 31-1329) [17]. The peak at 10.2° was assigned to the 001 plane of Na2Ti3O7 for TONTs powder before washing with HCl. The crystals of the nanotubes uncalcined are not very fine.

In the XRD spectra of the sample obtained by acid treatment (Fig. 5 for TONTs powder after washing with HCl), this peak cannot be seen clearly. In comparison to the as-synthesized sample, the intensity of the peak at 2□ = 24.2° of the acid treatment sample increased, but that of peak at 28.4° decreased. These differences can be explained by the exchange from Na2Ti3O7 to H2Ti3O7 [19, 20], and the XRD spectra of the calcinated sample i.e. TONTs-N2 powder with strong diffraction peaks completely differ from those of uncalcinated sample. The patterns at 2□ ≅ 25.4°, 37. 9°, 48.1°, and 62.8° clearly present the anatase

phase TiO2 of nanotubes indicating the transformation from titanate into anatase phase in the wall of TiO2 nanotubes after calcination at 450 °C for 3h [21, 22]. The XRD data showed the presence of sodium titanate phase Na2Ti3O7 of the as-prepared sample as well as the protonated titanate phase H2Ti3O7 of acid treatment sample and anatase phase of calcinated sample. These results indicated an ionic exchange from Na+ to H+ after washing treatment process as well as a phase transformation from titanate into anatase phase after calcination process.

Fig. 5 shows the XRD patterns taken from initial TONPs (precursor) and photo catalyst with HCl washing to pH=7. In the pH-decreasing course with HCl washing of pH= 6.5 to 7, there are characteristic peaks positioned at 2□ = 24° and 28°. These peaks have been assigned to the diffraction of titanates such as Na2Ti2O5.5H2O, Na2Ti3O7. lepidocrocite titanates. The amount of H+ ions provided from the acid may not be enough to replace the Na+, therefore the formation catalytic powders are still the structure with titanate not titanium dioxide.

Concerning palladium, the presence of Pd nanoparticles is indicated via diffraction peaks appearing at 2□ values of 40.1 and 46.7°. They were assigned to the (111) and (200) crystal plane spacing's of face-centered cubic (FCC) Pd (JCPDS no 46-1043, respectively. Only two peaks of three peaks that designated Pd were observed. This was since one peak overlaps with the anatase TiO2 at 2□ = 68.1 (220).Hence, these diffraction peaks further signifies the metallic state of the loaded Pd nanoparticles.

Fig. 6 shows nitrogen adsorption-desorption isotherms of Pd-TONTs-N2 powder expressed by relative pressure (P/P°) vs. cc/g (Volume @ STP) and their pore size distribution (inset) i.e. (N2-physiosorption isotherm and pore size distribution).

As seen in Fig. 6, the nitrogen sorption isotherm is of type (IV), characteristic for TONTs materials. It displays a pronounced capillary condensation step of 0.4 to 0.98 P/P°. The Pd-TONTs-N2 material has a BET surface area of 177 m2/g and a total pore volume of 0.389cm3/g. It has a bimodal pore size distribution with maxima around 3.94 and 7.59 nm in case of (Diameter (nm) vs. dv (d) cc/nm/g (Fig. 6 b).

The nitrogen adsorption-desorption isotherms and corresponding pore size distribution of the synthesized samples are illustrated in Fig. 6 a and b. As can be seen, all the samples have a stepwise adsorption and desorption hysteresis, represented via type-IV isotherms, with the characteristics of a mesoporous material [23]. The differences in BET surface area, average pore size and pore volume after Pd desorption is summarized in Table 1. Additionally, the average pore diameter, determined through the Barrett-Joyner-Halenda

(BJH) method by the adsorption isotherm (Fig. 6 b) was found to decrease after the adsorption of Pd NP. The decrease of BET surface area and average pore diameter was owing to a slight blocking of the pore in anatase TONTs-N2 by the deposited Pd NPs [24].

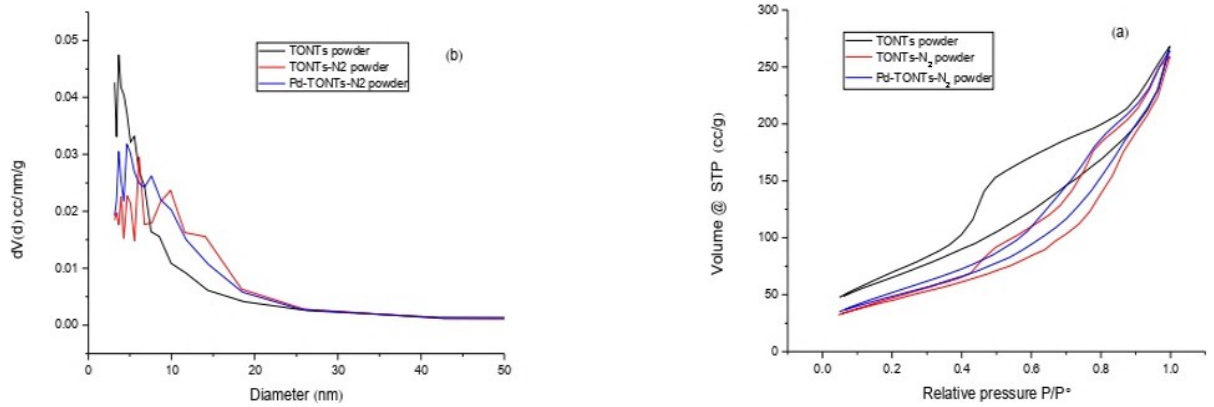

Fig. 6: (a) Adsorption–desorption isotherm of TONTs powder, TONTs-N2 powder and Pd-TONTs-N2 powder (b) the average pore diameter, determined through the Barrett-Joyner-Halenda (BJH) method by means of the adsorption isotherm.

Table 1: Shows the average pore diameter, determined through the Barrett-Joyner-Halenda (BJH) method using the adsorption isotherm. From Table 1, it is noted that diameter (nm) of Pd-TONTs-N2 powder catalyst (4.644 nm) is lower than that of Pd-TONPs-N2 powder catalyst (2.951 nm) [1]. And also the surface area of the synthesized catalysts (TONTs powder) are two to three times (2.2 times) larger than TONPs powders.

The BET surface area of the sample prepared with 10 M NaOH concentration is presented in Table 1. The average BET surface area of TONTs was 241.4 m2/g at 10 M NaOH concentration. These results showed that the surface area had

relation to the number and the length of the nanotubes, and they

were in good agreement with the nanostructures determined using the TEM method.

The surface area of catalyst with rinsing pH of 7 slightly upgrades to 241.4 m2/g because of the shortage in H+ ions. The amount of H+ ions provided from acid rinsing may not be enough to replace Na+, therfore the formation of catalytic powders are still lamellar structure not tubular. When the pH value of catalysts during the acid washing process is controlled to 2.2 further, the proportion of Na+ ions within the titanate would be decreased due to the increasing of the washing acidity (H+). The percent of the generated TiO2 nanotube would be also

increased by scrolling the lamellar titanate or titanium oxide sheets into tubullar structure. So the specific surface area can be up to 294.9 m2/g [17].

Table 1: The BET surface area, average pore size and pore volume of TONTs , TONTs-N2 and Pd-TONTs-N2 powde

	BET surface area (m^2/g) dsorption	Average pore size (Pore diameter) dv(d) (nm)	Porevolume(cm^3/g)
TONTs powder	241	3.647	0.363
TONTs-N_2 powder	170	6.102	0.38
Pd-TONPs-N_2 powder	98	2.951	0.247[1]
Pd-TONTs-N_2 powder	177	4.644	0.389

3.2 Methanol oxidation of Palladium supported on TONTs-N2 powder

Fig.7 shows the effect of loading for Pd-TONTs-N2 powder catalyst. It is clear that the catalytic current density increase with 1 µL and 3 µL respectively. Then when the loading 5 µL, the catalytic current density will decrease because of blocking of catalyst and also physical detaching. For 3 µL Pd-TONTs-N2 powder, the value of If/Ib was 3.21 which are larger than that reported for Pt/carbon (0.75) [25] i.e. it is about 4.28 times higher than that reported for Pt/carbon (0.75).

It is observed from Table 2 that If/Ib value of 3 µL Pd-TONTs-N2 powder catalyst is larger than that of 5 µL Pd-TONTs-N2 powder catalyst and 1µL Pd-TONTs-N2 powder catalyst respectively, indicating that 3 µL Pd-TONTs-N2 powder catalyst has the highest catalytic activity and current density.

A low If/Ib ratio points to poor electro oxidation of methanol to carbon dioxide during the forward scan, and too much accumulation of carbonaceous intermediates on the catalyst surface [26]. High current density and low Ib/If were achieved, which can be ascribed to the large surface area, reduced diffusion resistance, and excellent poisoning tolerance.

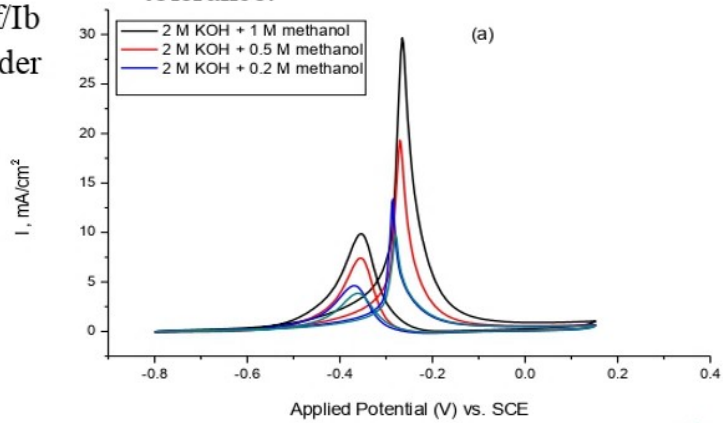

Fig. 7: Effect of loading for Pd-TONTs-N2 powder catalyst loaded on 3 mm Au working electrode in (2 M KOH + 1M methanol) at a scan rate was 50mV/s.

Fig. 8 shows CV of 3 µL Pd-TONTs-N2 powder loaded on 3 mm Au polycrystalline working electrode in 2 M KOH solution was baseline but in (2 M KOH + 1 M methanol) the catalytic current density increase.

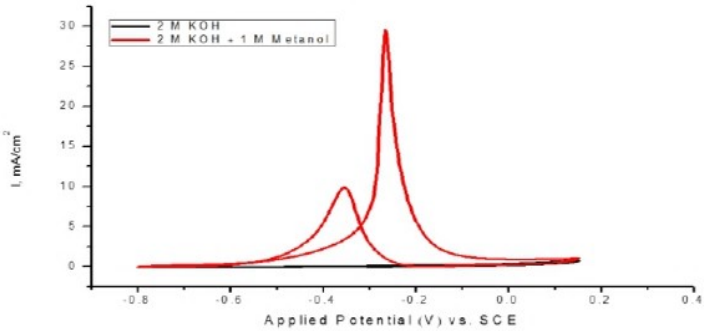

Fig. 8: CV of 3 µL Pd-TONTs-N2 powder loaded on 3 mm Au polycrystalline working electrode in 2 M KOH and in (2 M KOH + 1 M methanol) at a scan rate was 50 mV/s.

Table 2: Ip (peak height –mA/cm2) for both the forward and backward

paths also contains the values of If/Ib for the Pd@TONTs-N2 powder catalyst loaded on 3 mm Au polycrystalline working electrode 50 cycles for (MOR).

Loading (µL)	I_f(Peak height) (mA/cm^2) For forward	I_b (Peak height) (mA/cm^2) For backward	I_f/I_b
(1 µL)	24.43	7.82	3.12
(3 µL)	29.64	9.24	3.21
(5 µL)	15.26	6.76	2.26

Fig. 9 (a) indicates to palladium supported on titanium oxide nanotubes as catalyst for methanol oxidation reaction (MOR).

Fig. 9 (a) shows the electro catalytic activity for methanol oxidation reaction i.e. shows the CVs of the 3 µL Pd-TONTs-N2 powder catalyst in (1 M methanol+ 2 M KOH). It is clear from Fig. 9 that 1 M concentration of methanol gives high current density in contrast with other concentrations of methanol in basic medium of 2 M KOH.

In Fig. 9 (a), concerning the 1 M methanol concentration in basic medium, the peak current densities in the forward scan for Pd-TONTs-N2 powder catalyst were measured to be 29.64mA/cm2 in alkaline medium whereas the peak current densities in the backward scan were measured to be 9.24mA/cm2 (scan rate was 50mV/s). It is noted that the peak current is enhanced for catalyst prepared by photodeposition of PdCl2 on TONTs-N2 powder as support/catalyst using 0.3 M isopropanol as solvent.

Also the oxidation current has been normalized to specific current density so that the current density (I) can be directly used to compare the catalytic activity of the samples. The Pd-TONTs-N2 powder catalyst which was examined show a significantly improved methanol oxidation activity as compared to TONTs-N2 powder catalyst and Pd-TONPs-N2 powder.

The ratios of peak currents associated with the anodic peaks in forward (If) and backward (Ib) is generally used to describe the tolerance of a catalyst to intermediates generated during the methanol oxidation [27]. A low If/Ib ratio indicates poor

electro oxidation of methanol to

carbon dioxide during the forward scan, and excessive accumulation of carbonaceous intermediates on the catalyst surface [26]. For Pd-TONTs-N2 powder, the value of If/Ib was 3.21 which is larger than that reported for Pt/carbon (0.75) [25] i.e. it is about 4.28 times higher than that reported for Pt/carbon (0.75) and Pd/carbon. The results of If/Ib ratio indicates that Pd-TONTs-N2 powder (3.21) catalyst exhibit excellent poison tolerance than that of the Pd-TONPs-N2 (2.88) catalyst. The Pd-TONTs-N2 catalyst was an excellent electro catalyst compared to the other catalysts analysed, since it yielded the largest forward peak current density and a higher real surface activity, exchange current density and If/Ib ratio. That was in the case of 1 M methanol at a scan rate was 50mV/s. Fig.9 (b) shows the concentration (M) vs. Ip (peak height in mA/cm2) for both the forward and backward paths. The concentration is directly proportional to the peak height of forward and backward respectively and the relation between them is linear

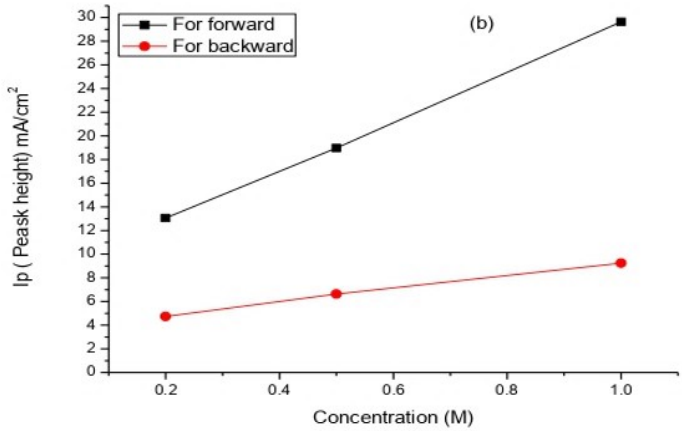

Fig.9: (a) Effect of concentration of methanol on 3 microliter Pd-TONTs-N2 powder loaded on Au polycrystalline working electrode in 2 M KOH at a scan rate was 50mV/s by current density (b) the concentration (M) vs. Ip (peak height –mA/cm2) for both the forward and backward paths.

Table 3: lists the values of If, Ib, and If/Ib for Pd-TONTs-N2 powder catalyst. It is observed

that Pd-TONTs-N2 powder with 1 M methanol concentration in basic medium of 2 M KOH have If/Ib value higher than that of 0.5 M and 0.2 M methanol concentration in basic medium of 2 M KOH, indicating that Pd-TONTs-N2 powder with 1 M methanol concentration in basic medium of 2 M KOH have higher catalytic activity

Table 3: The concentration (M) vs. Ip (peak height –mA/cm2) for both the forward and backward paths also contains the values of If/Ib for the Pd@TONTs-N2 powder catalyst loaded on Au polycrystalline working electrode 50 cycles.

Concentration (M) of ethanol	I_f (Peak height) (mA/cm^2) For forward	I_b (Peak height) (mA/cm^2) For backward	I_f/I_b
0.2	13.06	4.73	2.76
0.5	18.97	6.64	2.86
1.0	29.64	9.24	3.21

Fig. 10 shows the effect of the scan rate for methanol oxidation process at Pd-TONTs-N2 powder catalyst in 2 M KOH in the presence of 1 M methanol. The curve shows that the anodic current for methanol oxidation at Pd-TONTs-N2 powder catalyst increases rapidly with increasing the potential scan rate and anodic potential shift toward higher potential values. Indeed the time window for methanol oxidation process at higher scan rates becomes very narrow where facile electron transfer takes place between methanol and catalytic sites. The proportionality of anodic peak currents to the scan rate in a range of 1-150 mV/s was illustrated in Fig. 10. The anodic peak current are linearly proportional to the scan rate suggest that the overall oxidation of methanol at this electrode is controlled by the diffusion of methanol from solution to surface redox sites [28, 29].

Fig. 10 shows the effect of scan rate for Pd-TONTs-N2 powder electrode in a potential range from (-0.8 V to 0.15 V) recorded at different scan rate for 1 M methanol in basic medium (2 M KOH) solution, Fig. 10 also shows an enhanced anodic peak current that increase linearly with increasing scan rate, this behavior is characteristic of an electrochemical reaction controlled by a diffusion process.

The mass loading of Pd in 3 µL Pd-TONTs-N2 powder is equals to 0.0225 mg Pd, this value was determined by ICPS-7000.

A low If/Ib ratio indicates poor electrooxidation of methanol to carbon dioxide during the forward scan, and excessive accumulation of carbonaceous intermediates on the catalyst surface.

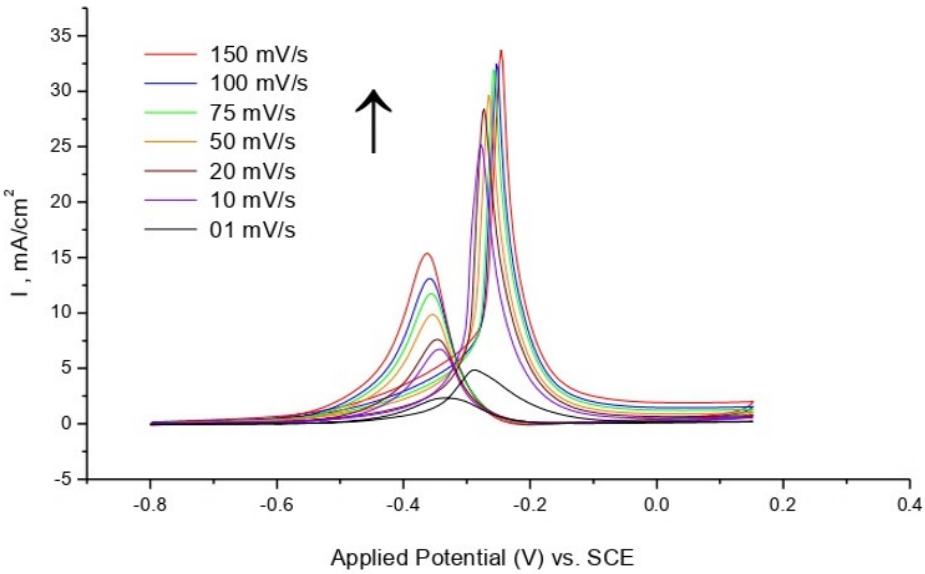

Fig. 10: CV for Pd-TONTs-N2 powder loaded on 3 mm diameter Au polycrystalline working electrode in (2M KOH+1M methanol), 3 microliter loading by current density, 50cycles (effect of scan rate).

Fig. 11 shows the chronoamperometry (CA) of Pd-TONTs-N2 powder loaded on 3 mm diameter Au working electrode in (2 M KOH+ 1M methanol) at different potentials (-0.4 V,-0.27 V and 0 V). At the principal step of the chronoamperometry curves, the current density is comparatively high because of the adhesion of methanol molecules on the active sites. Then the current density decrease when the time increases. Approximately 200 s later, the curve becomes stable. The stable current density of the Pd-TONTs-N2 powder at the potential -0.27 V is the highest among the other potentials -0.4 V and 0 V, signifying that this would achieve equilibrium among catalytic activity and poison resistance owing to suitable deposition quantity of Pd nanoparticles on titanium oxide nanotubes. Chronoamperometry (CA) is an electrochemical method in which the potential of the working electrode is stepped and the resultant current from faradaic process happening at the electrode (produced by the potential step) is monitored as a function of time)

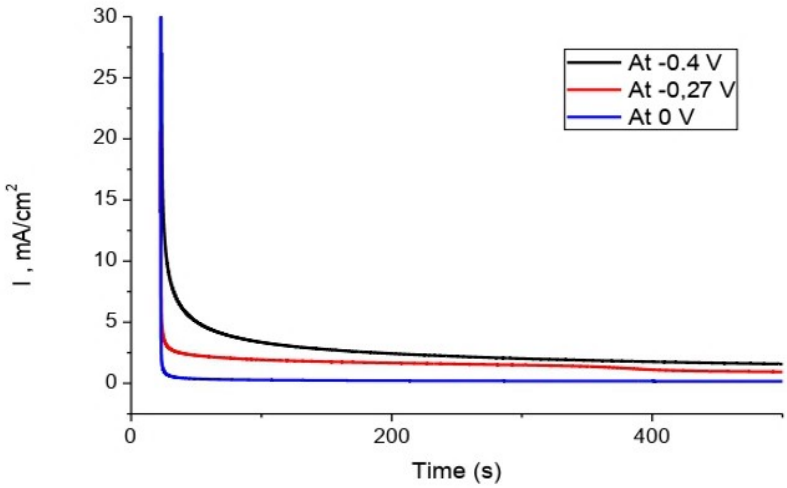

Fig. 11: Chronoamperometry (CA) for Pd-TONTs-N2 powder loaded on 3 mm diameter Au polycrystalline working electrode in (2 M KOH+ 1M methanol).

Fig. 12 shows the catalytic stability of the Pd-TONTs-N2 powder catalyst from first cycle to 50 cycles in (2 M KOH + 1 M methanol) with a scan rate was 50mV/s. Stability test was performed for Pd-TONTs-N2 powder catalyst. Fig. 12 shows the CVs for Pd-TONTs-N2 powder catalyst after continuous cycling between -0.8 V and 0.15 V for a total of 50cycles.

The catalytic stability of Pd-TONTs-N2 powder catalyst for methanol oxidation was investigated via CV as shown in Fig. 12.The Pd-TONTs-N2 powder methanol oxidation current shows a steady decrease in current density within the first few cycles (10 cycles) and then a nearly constant current density was progressively established for longer time. Therefore, the results reveal that Pd-TONTs-N2 powder possesses higher catalytic activity and stability than Pd-TONPs-N2 powder in alkaline media.

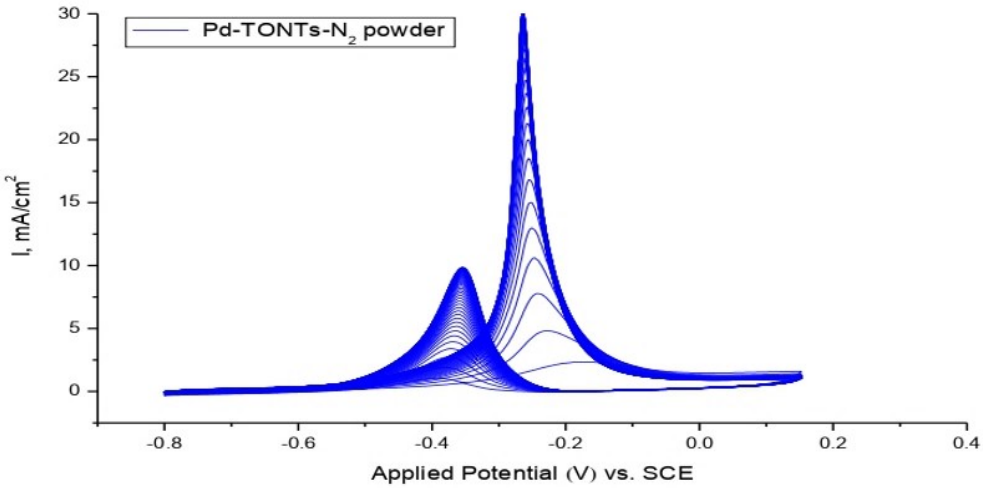

Fig. 12: CV of $3\mu l$ Pd-TONTs-N2 powder, from 1 cycle to 50 cycles loaded on Au working electrode as baseline, all in (2M KOH+1M methanol) at a scan rate was 50 mV/s by current density.

It is noted that the ratio If/Ib of Pd-TONTs-N2 powder is about 4.28 times higher than that stated for Pt/carbon (0.75), 1.43 times higher than that stated for Pd/TiO2 Nano belts, 2.77 times higher than that stated for Pd/AC activated carbon, 3.53 times higher than that stated for Pd/TiO2 nanobelts-C, and 1.12 times higher than that stated for Pd-TONPs-N2 powder.

That is to say, the Pd-TONTs-N2 powder elector catalyst exhibits better poison tolerance and about four to three times methanol oxidation current density higher than that reported for Pt/C and Pd/C catalysts respectively. This was attributed to synergistic effect on TONTs support Pd NPs and on CO oxidation, the ordered unidirectional structures of TONTs and the greater conductivity and electrochemical active surface area of TONTs-N2 powder.

Table 4: The composition of the If/Ib ratio for the 3µL catalysts loaded on Au polycrystalline working electrode at a scan rates was 50mV/s for (MOR).

Catalysts	I_f (mA/cm^2)	I_b (mA/cm^2)	Mass loading of Pd in (mg/ml)	I_f/I_b
Pd-TONPs-N_2 powder	21.3	7.4	0.0555 in 3 µL	2.88[1]
Pd-TONTs-N_2 powder	29.64	9.24	0.0225 in 3 µL	3.21
Pt/C	0.75	1.0	……	0.75[25]
Pd/TiO_2 Nano belts	2.57	1.14	0.523 in 3 µL	2.25[30]
Pd/AC Activated carbon	2.9	2.5	0.353 in 3 µL	1.16[30]
Pd/TiO_2 nanobelts-C	4.0	4.4	0.3348 in 3 µL	0.91[30]

4. Conclusions

TONPs and TONTs supports do not suffer from degradation and the metals as catalysts can be deposited on its surfaces compared to carbon support by photodeposition method. The Pd NPs showed the smallest particle size, very well dispersion on TONTs-N2 powder, higher electrochemical active area and stability as compared to Pd-TONPs-N2 powder , Pt/C and Pd/C because it yielded the largest forward peak current density and higher real surface activity, exchange current density and If/Ib ratio. The Pd-TONTs-N2 powder electrode showed the highest electrocatalytic activity towards the MOR. In addition the cycle tests proved that Pd-TONTs-N2 powder catalyst has the highest current density and the lowest decay rate for current density compared with the Pd-TONPs-N2 powder. The addition of Pd NPs ontoTONTs-N2 powder leads to the improvement of electrocatalytic activity. Therefore, the Pd-TONTs-N2 powder elector catalyst has higher electrochemical active area and higher catalytic activity for MOR compared with Pd-TONPs-N2 powder catalyst.

5. Acknowledgements

The author (Mohammed .A .H . Awad) would like to utilize this opportunity to express his gratitude to Professor Nabil Alkadasi for his non-stop guidance; support throughout the last two years.

6. References

[1] Nabil AN Alkadasi, MA Awad, MA Ghanem, AM Al-Mayouf. Palladium supported on titanium oxide nanoparticles as a catalyst for methanol oxidation reaction. International Journal Of Chemistry Studies. 2018: 2(3):10-16.

[2] M.S. Sander, M. J. Coˆte´, W. Gu, B. M. Kile, C.P. Tripp. Adv. Mater. 16 (2004) 2052–2057.

[3] Q. Chem, W. Z. Zhou, G. H. Du, L. H. Peng, Adv. Mater. 14 (2002) 1208–1211.

[4] Y. Chen, J. C. Crittenden, Hackney S , L. Sutter, and D. W. Environ Sci Technol .39 (2005) 1201–1208.

[5] Y. Zhang, Fu. W, H .Yang Qi .Q, Zeng Y, Zhang T, Ge. R, Zou. G. Appl Surf Sci .254 (2008) 5545–5547.

[6] R.P. Vitiello, J. M. Macak, A. Ghicov, H. Tsuchiya, L.F.P. Dick, P. Schmuki, Electrochem. Commun. 8 (2006) 544–548.

[7] Z. Y .Yuan, B.L Su. Colloids Surf A .241(2004) 173–183.

[8] Y. Ma, Y. Lin, X. Xiao , X. Zhou and X. Li. Mater Res Bull 41(2006) 237–243.

[9] N. S. Viriya-empikul, T. Charinpanitkul, T. Kikuchi, W. Tanthapanichakoon. Nanotechnology. 19 (2008) 035601.

[10] K. Rajeshwar, M. E. Osugi, W. Chanmanee, C. R. Chenthamarakshan, M. V. B. Zanoni, P. Kajitvichyanukul, R. Krishnan-Ayer, J. Photochem. Photobiol.C. 9 (2008) 171–192.

[11] M. D. Hernández-Alonso, F. Fresno, S. Suárez, J. M. Coronado. Energy Environ. Sci. 2 (2009) 1231–1257.

[12] H. Chen, L.Wang. Beilstein J.Nanotechnol. 5 (2014) 696–710.

[13] D. B. Ingram, S. Linic. J. Am. Chem. Soc. 133 (2011) 5202–5205.

[14] L. Jiang, G. Zhou, J. Mi, Z. Wu. Catal. Commun. 24 (2012) 48–51.

[15] C. L Wong, Y. N Tan, A. R Mohamed. J Environ Manage. 92 (2011)1669–1680.

[16] Cui L, Hui KN, Hui KS, Lee, S.K, Zhou, W, Wan Z.P and Chi-Nhan Ha Thu .Mater Lett .75 (2012) 175–178.

[17] Yu Zhen Zeng, Yu Chang Liu, Yun Fang Lu, and Jen Chieh Chung. International Journal of Chemical Engineering and Applications, 5 (2014) 234-239.

[18] Thu Ha Thi Vu ,Hang Thi Au , Lien Thi Tran , Tuyet Mai Thi Nguyen , Thanh Thuy Thi Tran ,Minh Tu Pham , Manh Hung Do , Dinh Lam Nguyen . Journal of materials science, 49 (2014) 5617-5625.

[19] Xu H, Zhang Q, Zheng CL, Yan W, Chu W. Appl Surf Sci. 257 (2011) 8478–8480.

[20] Shi L, Cao L, Liu W G. Su, R. Gao, and Y. Zhao.Ceram Int 40 (2014) 4717–4723.

[21] Michailowski A, AlMawlawi D, Cheng G and M. Moskovits. Chem Phys Lett 349 (2001)1–5.

[22] Seo DS, Lee JK, Kim H . J Cryst Growth, 229 (2001) 428–432.

[23] Pan, X.; Xu, Y.-J. Appl.Catal. 459A (2013) 34–40.

[24] X. Pan, Xu, Y.-J. J. Phys. Chem.C. 117 (2013) 17996–18005.

[25] K. Nukumizu, J. Nunoshige, T. Takata, J.N. Kondo, M. Hara. Chem. Lett. 32 (2003) 196-197.

[26] J.J. Wu, H.L. Tang, Z.H. Wan, W.T. Ma. Electrochim. Acta , 54 (2009) 1473-1477.

[27] Y.N. Wu, S.J. Liao, Z.X. Liang, L.J. Yang, R.F. Wang. J. Power Sources 194 (2009) 805-810.

[28] Allen J. Bard. John Wiley and Sons Inc, New York, (2001) L.R.F.

[29] T.S. De Gromoboy, L.L. Shreir, Electrochim. Acta 11 (1966) 895-904.

[30] Robert Liang, Anming Hu, John Persic, Y.Norman Zhou. NANOMICRO LETTERS. 5 (2013) 202-2012

الترسيب الضوئي للبلاديوم المحمل على مسحوق أنابيب نانوية لثاني أكسيد التيتانوم كحفاز كهربائي لتفاعل أكسدة الميثانول

أ.محمد أحمد حسين عوض ، أ.د. نبيل عبدالله القدسي ، أ.د. عبدالله محمد المعيوف

الملخص:

تم تحضير مسحوق أنابيب نانوية لثاني أكسيد التيتانوم كمدعم حفاز بوساطة المعالجة الحرارية المائية، وباستخدام مسحوق جزيئات أكسيد التيتانيوم النانوية، ومن ثم المعالجة الحرارية في جو من النيتروجين عند درجة حرارة 450 درجة مئوية، ولمدة ثلاث ساعات للحصول على مسحوق كمدعم حفاز ثم تحميل فلز البلاديوم عليه بوساطة تقنية الترسيب الضوئي وباستخدام كلوريد البلاديوم والإيزوبروبانول (TONTs-N2) بمساحة سطحية عالية بلغت 177 م2/جرام-Pd) .
(TONTs-N2 كمانح للإلكترونات. إذْ تم الحصول على الحفاز

تم إجراء التوصيفات الفيزيائية اللازمة بوساطة حيود الأشعة السينية و المجهر الإلكتروني الماسح والمجهر الإلكتروني النفاذ وكذلك مساحة السطح وتحليل حجم المسامات. وتم دراسة السلوك الكهروكيميائى والحفزى باستخدام التوصيف الكهروكيميائى وبدراسة منحنيات مسح الجهد الدورى وكذلك منحنيات الوقت مع التيار في محلول قاعدي من الميثانول.

فعالية كهروكيميائية تجاه تفاعل أكسدة الميثانول في وسط قاعدي وهذا القطب له كثافة تيار عالية Pd-TONTs-N2 ولقد أظهر القطب فاعلية سطحية أعلى ونسبة التيار الأمامي إلى الخلفي عالية. وأثبتت النتائج أنه الأكثر نشاطا مع حيث كثافة التيار، والأقل من حيث الجهد اللازم للأكسدة، ولديه استقرار على المدى الطويل نسبيًا لأكسدة الميثانول لذا يمكن استخدامه كحفاز واعد لخلايا الوقود .

كلمات مفتاحية:

تفاعل أكسدة الميثانول، مسحوق أنابيب نانوية لثاني أكسيد التيتانوم، الترسيب الضوئي، البلاديوم كحفاز كهربائي، منحنيات الوقت مع التيار